JOURNAL OF AIRCRAFT
Vol. 30, No. 1, Jan.–Feb. 1993

Mechanisms of Transonic Blade-Vortex Interaction Noise

H.-M. Lent,* G. E. A. Meier,† K. J. Müller,‡ F. Obermeier,§ U. Schievelbusch,‡ and O. Schürmann‡
Max-Planck-Institut für Strömungsforschung, 3400 Göttingen, Germany

Experimental investigations of aerodynamic sound generation due to vortex-airfoil interaction in two-dimensional transonic flow were performed using two different experimental set ups—a vacuum-operated transonic wind tunnel and a shock tube. Flow visualization was accomplished by a Mach-Zehnder interferometer as well as by a holographic interferometer. The interferograms obtained were evaluated by an image processing system. In addition, pressure measurements were carried out in the shock tube which allows for a correlation of time-dependent pressure distributions and the density distributions evaluated from the interferograms. Two mechanisms of aerodynamic sound generation are identified. These are different from the dipole-like mechanism known for subsonic flowfields. The newly found sound waves are called "transonic waves" and "compressibility waves." For both of them simple models have been suggested which can partly explain their occurrence and their strengths.

I. Introduction

THE blade-vortex interaction (BVI) noise[1] is a primary component of helicopter noise and consists of periodically emitted, impulsive-like signals which are caused by the transonic interaction of rotor blades with the tip vortices shed from preceding blades. To reduce this kind of noise it is necessary to understand the physical mechanism of the interaction and identify the important parameters affecting the sound generation.

Until now, there seems to be no analytical description available in literature which gives sufficiently reliable results for the radiated sound field, especially if flow separation at the rotor blades affects the flowfield. One of the main difficulties is due to the fact that in transonic flows the actual source region cannot be regarded as a compact one. Therefore, the ordinary theories valid for subsonic compact flow cannot be applied (e.g., Möhring et al.[2]). Furthermore, the equations of a generalized theory developed independently by Ffowcs Williams and Hawkings[3] and Möhring et al.[4] are of no real help here as they have to be regraded as integral equations. Their actual solution requires detailed knowledge on rotor aerodynamic loads and flowfield information.

There are, however, numerical calculations on compressible BVI noise known in the other studies.[5–8] References 7 and 8 validate our experimental work set forth in the present article.

On the experimental side of the problem there are the measurements which were performed in a full three-dimensional, compressible flow.[1,9] They are useful to get an overall estimation of the radiated noise but are less-suitable to discover and understand the basic mechanisms of BVI noise. In addition, visualization techniques were applied to investigate BVI in low-speed tunnel flows (e.g., Haertig et al.[10]).

To our knowledge, Meier and Timm[11] performed the first experiments that accounted for compressibility and simultaneously measured sound emission. A similar experiment was later performed by Mandella and Bershader[12] but they did not measure any sound emission.

During the last few years the authors have been interested in compressible BVI and in the different sound generation mechanisms which occur in such an unsteady flow.

Because the actual flow geometry is highly three-dimensional and unsteady and it seems to be nearly impossible to separate the different mechanisms of sound generation in this very complex flowfield, we have confined this investigation to simplified, two-dimensional flow geometries (Fig. 1).

The main experimental difficulty of these investigations has been the generation of a well-defined vortex in a compressible high-speed flow. Since it seemed impossible to generate the vortex with any mechanical devices—such as a sudden increase of the angle of attack of an airfoil—two other concepts were employed. First, the vortices of a von Kármán vortex street were used for the BVI in a vacuum operated, continuously running transonic wind tunnel and, second, the starting vortex of a lifting airfoil was used in a shock tube. Both setups have got their advantages and disadvantages. The wind tunnel allows measurements of long duration and the quality of the interferograms obtained is superior to the one from the shock-tube experiments. On the other hand, one does not get exact single vortex airfoil interactions; the interactions are somewhat spoiled by the preceding and following vortices, respectively. In addition, due to the special shape of the side walls of the wind tunnel (Fig. 2), it is not quite clear how to define an unambiguous characteristic Mach number of the steady mean flow. The shock-tube experiments allow mea-

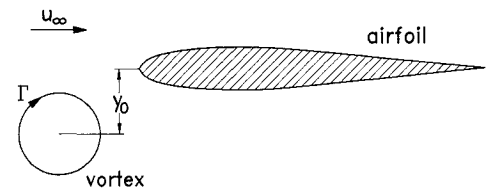

Fig. 1 General flow configuration.

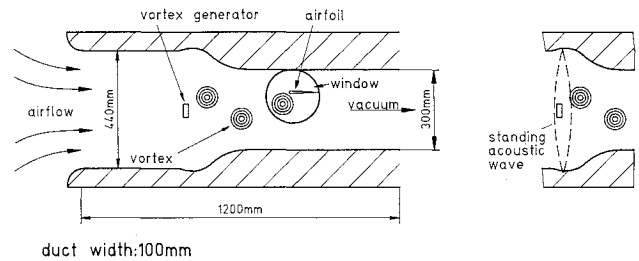

Fig. 2 Test section of the transonic wind tunnel.

Presented as Paper 90-3972 at the AIAA 13th Aeroacoustic Conference, Tallahassee, FL, Oct. 22–24, 1990; received Jan. 28, 1991; revision received Jan. 30, 1992; accepted for publication Jan. 31, 1992.

*Research Scientist, Bunsenstraße 10.
†Professor; currently Direktor des Instituts für Experimentelle Strömungsmechanik der DLR Göttingen.
‡Graduate Research Fellow, Bunsenstraße 10.
§Professor, Bunsenstraße 10.

surements with single vortices. Their cores are rather small, therefore, they behave similarly to line vortices. Unfortunately, the flowfield of interest is blurred by shock wavelets resulting from reflections of the primary shock. In balancing both experiments we regard them in some ways as complimentary, and by means of both experimental setups we were able to improve the understanding of the generation of sound waves.

From experimental and theoretical investigations at least four different possible mechanisms of airfoil—vortex interaction noise are known:

1) The vortex noise when vortex filaments pass the airfoil at low Mach number: the generated sound field is well understood by means of a nonviscous, subsonic theory.[3,4,13]

2) Stalling and reattachment of the flow due to a varying effective angle of attack while a vortex passes an airfoil: the corresponding theoretical investigation requires inclusion of viscous as well as boundary-layer separation effects.[14]

3) Shock development due to compressibility effects when at high subsonic Mach numbers vortices cause an unsteady displacement of the stagnation point of the flow at the leading edge of an airfoil and generate an enlarged high-pressure region there: this high-pressure region then propagates upstream and steepens to shock waves. These shock waves will be called "compressibility waves."

4) Shock development due to unsteady and locally confined supersonic flow regions along the shoulder of the airfoil: the emitted shock waves will be called "transonic waves."

In the present article we will concentrate mainly on the latter two mechanisms.[15,16]

II. Experimental Setup

A. Wind Tunnel

The test-section dimensions of the transonic wind tunnel used in this study (Fig. 2) are: 100-mm span and 300-mm height, the length can be varied between 600–1200 mm. The tunnel side walls contain 230-mm-diam windows of interferometric quality for observation purposes. Most experimental data were obtained by using a Mach-Zehnder interferometer with a field-of-view of 160 × 110 mm^2. Since the flow is unsteady, either a high-speed drum camera or a Cranz-Schardin camera were used. The drum camera takes 200 pictures with a framing rate of 10 kHz. Since this framing rate is not high enough to resolve some fast effects during the transonic BVI, a Cranz-Schardin camera was built[17] which allows eight pictures to be taken with a framing rate of up to 200 kHz. This camera consists of eight CCD cameras connected with an eight-image storing device which provides quick access to the pictures. As a light source, for both the drum camera and the Cranz-Schardin camera, pulsed LEDs were used. Measuring plates with an array of pressure transducers could also be mounted in place of the windows in the tunnel walls.

The vortices were generated as a von Kármán vortex street behind a rectangular cylinder. They interact downstream with an airfoil. Here, in most of our experiments, vortices of the upper row of the von Kármán vortex street (clockwise-rotating vortices) moved below the airfoil. To approximately confine these interactions to single vortices, a sufficiently large distance between two oncoming vortices is needed. For that purpose the height of the tunnel section in which the vortices are generated has been enlarged. This allows for a vortex separation from the cylinder at a rather small local Mach number which implies small separation frequencies. In addition, the flow is accelerated ahead of the test section to stretch the vortex row even further. Finally, a very well-developed von Kármán vortex street with a constant separation frequency is obtained for discrete Mach numbers by an acoustic feedback, due to a standing sound wave normal to the mean flow direction; this is very much like a Parker mode.[18,19]

In the experiments the flow Mach number was varied between 0.4–0.9, the circulation of the vortices was between 5–40 m^2/s, and the clearance distances at which the vortices pass the airfoil were between 10–40 mm. In addition, the shape and the size of the airfoil were varied as well. In the wind tunnel, test-run duration of up to 20 s (depending on the flow Mach number and the cross section) can be achieved.

B. Shock Tube

To investigate the interaction of a single vortex with an airfoil, a special shock tube (Fig. 3) was used. For flow visualization purposes, the shock-tube test section was designed to have parallel side walls while the upper and lower walls are slightly curved to minimize effects due to reflections of the primary shock. Its cross section in the low-pressure side is 100 × 700 mm^2. The pressure ratio (p_4/p_1) between the driving section and the test section can be varied between 1–40; most experiments were performed with $p_4/p_1 = 13$ which leads to a shock strength of $p_2/p_1 = 3.2$ and a flow Mach number M_2 behind the shock of 0.76.

For flowfield observation, a real-time holographic interferometer was constructed. The holograms themselves were taken by a thermoplastic film camera for instant recording and reconstruction.[20] A larger field-of-view (400 mm) was used in this setup since Plexiglas® (acrylic glass) windows of ordinary quality were acceptable. Pressure measurements were made simultaneously with the interferograms using pressure transducers mounted into the plexiglas window. This enabled a direct comparison between the pressure signals and the interferograms.

In the shock tube, first a strong shock wave moves into a medium at rest. Behind the shock a flow is induced. If the shock wave moves over a lifting airfoil the flow will create a circulation around it. In addition, a vortex is generated at the trailing edge of the airfoil to compensate for the circulation around it. By using different airfoils with different lifts the strength of the created vortex can be varied. A favorable feature of such a vortex is the fact that its core radius is rather small and that it may approximately be regarded as a potential vortex. After the vortex is generated at the trailing edge it moves in a manner close with the velocity of the flow induced

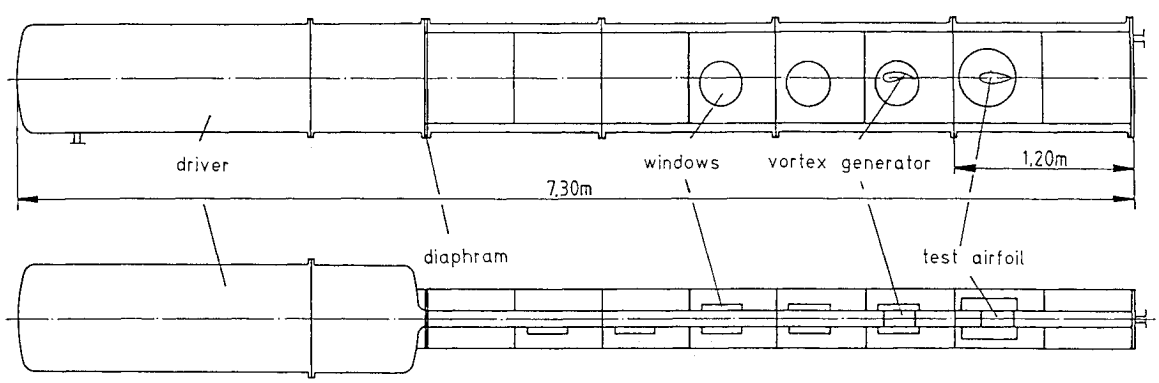

Fig. 3 Shock tube showing the general setup and cross section.

by the primary shock wave, and later interacts with a second airfoil. First, however, it interacts with the weak shock wave caused by the reflection of the primary shock at the second airfoil. Even though the vortex will be slightly affected by this interference we did not account for it in the evaluation of the experimental data.

III. Experimental Results

In the transonic flow regime at least two new mechanisms of aerodynamic sound generation by BVI could be identified. They seem to be fundamentally different from the dipole-like sound known from subsonic flows.

A. Compressibility Waves

The so-called compressibility waves caused by BVI have first been observed in the transonic wind tunnel. A typical time sequence of interferograms and the corresponding density distributions (which were evaluated semiautomatically by an image processing program developed in our institute[21]) are shown in Fig. 4. The parameters were: Mach number M = 0.66, a SC 1095-airfoil with chord length c = 120 mm, circulation of the incoming vortex Γ = 26 m²/s, and a framing rate of the drum camera 7.7 kHz.

On the first interferogram the vortex is directly below the leading edge of the airfoil (white arrow); the stagnation point has moved to the upper side. As the field-of-view is rather small, the vortex, which normally is represented by a system of concentric fringes on an interferogram, can only be seen at the lower edge of the picture. On the second picture the stagnation point has snapped back to its normal position, while in the flowfield a density maximum ahead of the leading edge becomes visible. Finally, on the third picture the density maximum starts to move upstream (black arrow), it becomes steeper at its front and weaker at its back.

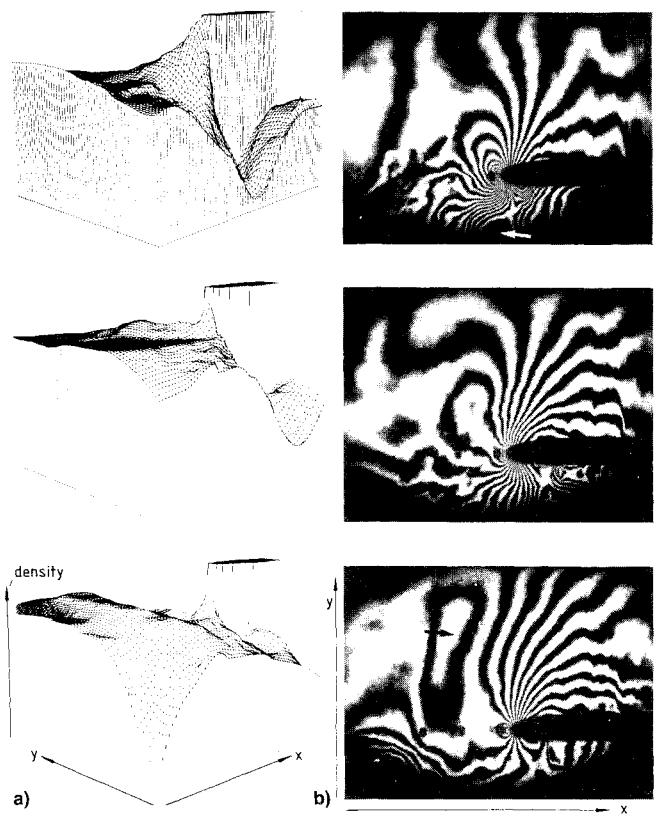

Fig. 4 Generation of a compressibility wave: Airfoil SC 1095, M = 0.66, Γ = 0.26 m²/s, c = 120 mm, framing rate 7.7 kHz; a) density distributions obtained by image processing; and b) interferograms. The arrow in the first interferogram indicates the location of the vortex and the arrow in the third one indicates the separated high-pressure region.

To investigate the influence of the airfoil's shape on this wave generation different airfoils were used. No significant differences could be observed and it seems primarily that the wave does not depend on the geometry of the leading edge as long as its thickness remains the same. By increasing the vertical distance between the vortex path and the profile, the wave becomes weaker. In contrast, at increasing Mach numbers the wave seems to get stronger. Below a Mach number of about 0.6 the wave is no longer visible on the interferograms. Since only the compressibility of the flow seems to govern the generation of this wave, it is called "compressibility wave."

Unfortunately, Fig. 4 shows only the near field of the BVI. Therefore, to get at least some idea on what may happen in the far field, the original airfoil was replaced by a smaller one (60-mm chord length). The corresponding interferograms shown in Fig. 5 were taken by the Cranz-Schardin camera with a framing rate of 35 kHz. The Mach number was M = 0.9 and the circulation Γ = 16 m²/s. Here the experiment was carried out at a higher Mach number as the steepening effects get more pronounced with the increasing Mach number. The pictures demonstate that the compression waves steepen up to weak shock waves which propagate upstream. The arrows included in the first interferogram point from right to left to the shock which corresponds to the leading edge of the high-pressure region separated from the nose of the airfoil, to the shock which is the steepened front of the compression wave caused by the preceding vortex, and to the shock which was generated by an even former vortex. Unfortunately, as these waves are partly disturbed by the vortex generator and by the incoming vortices, their directivity pattern cannot be obtained completely.

The compressibility wave has also been observed in the shock-tube experiments. A series of typical interferograms are shown in Fig. 6. Here, the flow Mach number is 0.76, the circulation of the vortex 19 m²/s. Thermal effects already yield

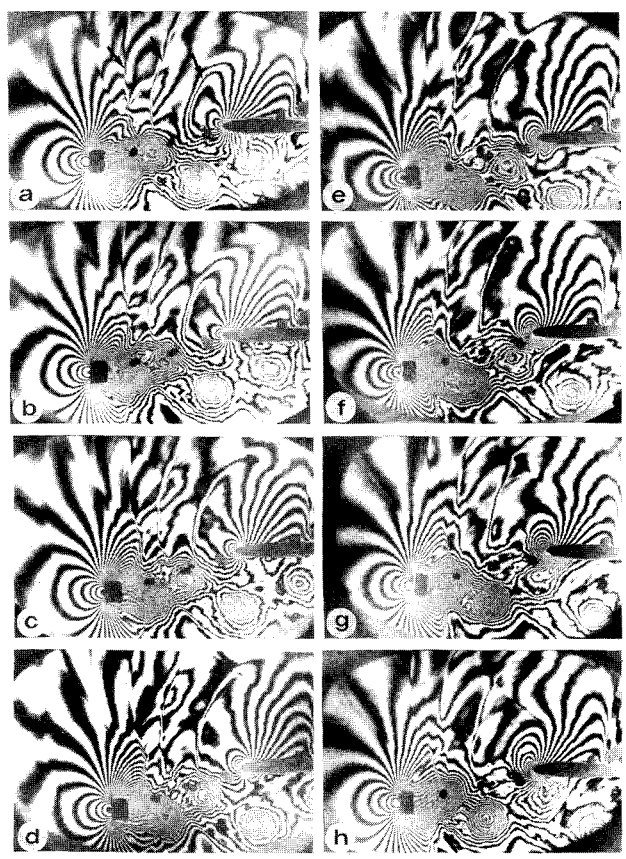

Fig. 5 Far field of compressibility waves: NACA 0012 airfoil, M = 0.9, Γ = 16 m²/s, c = 60 mm, and a framing rate 35 kHz. The arrows in interferogram (a) indicate the locations of compressibility waves.

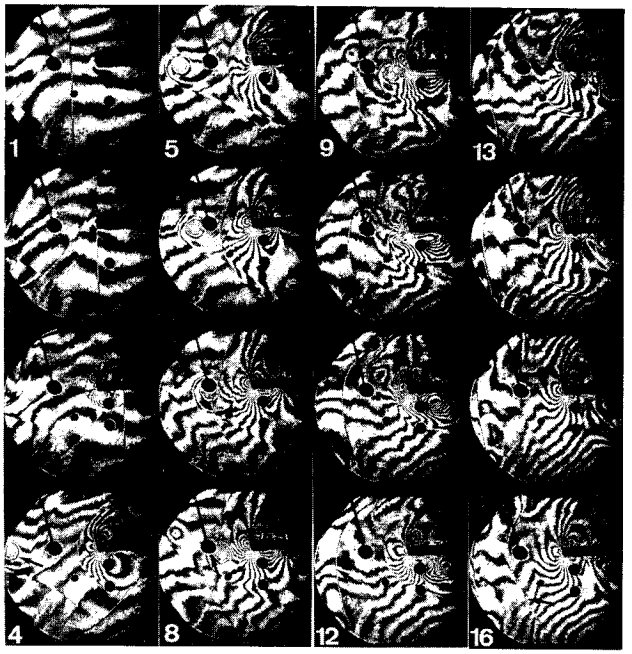

Fig. 6 Compressibility wave observed in the shock tube: $M = 0.76$ and $\Gamma = 19$ m/s, blunt body. The arrow in (4) indicates the vortex, in (8) the pressure transducer, in (12) the reflected wave, and in (16) the compressibility wave.

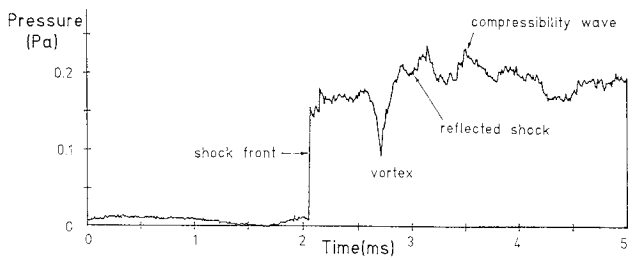

Fig. 7 Typical pressure signal measured by the pressure transducer (Fig. 6) just ahead of the blunt airfoil. $M = 0.76$, $\Gamma = 19$ m²/s.

some fringes on the interferogram where the flow is still at rest.

On the first picture of the interferograms the primary shock moves from left to right in front of the airfoil. On the fourth picture the vortex becomes visible (marked by an arrow), and on the seventh the shock is reflected from the airfoil. The interaction at the leading edge takes place only on the tenth and eleventh picture where a high-density region in front of the leading edge can already be observed. Although separation occurs at the lower side of the airfoil, and probably a secondary vortex is generated, this does not seem to affect the wave generation. On the fifteenth picture the compressibility wave passes a pressure transducer. The corresponding time-dependent pressure signal measured just ahead of the airfoil by the pressure transducer is shown in Fig. 7. Clearly seen are the pressure decreases when the incoming vortex passes the transducer (Fig. 6.7) and the pressure increases when the reflected shock (Figs. 6.8 and 6.9) and when the compressibility wave (Figs. 6.14 and 6.15) reach the transducer, respectively.

In additional experiments, the vertical position and the angle of attack of the airfoil generating the vortex were changed to vary the circulation of the vortex and vertical distance between the vortex path and the airfoil. We will come back to these results in Sec. IV.A.

B. Transonic Waves

A second mechanism of aerodynamic sound generation can be identified when due to the blade vortex interaction a locally

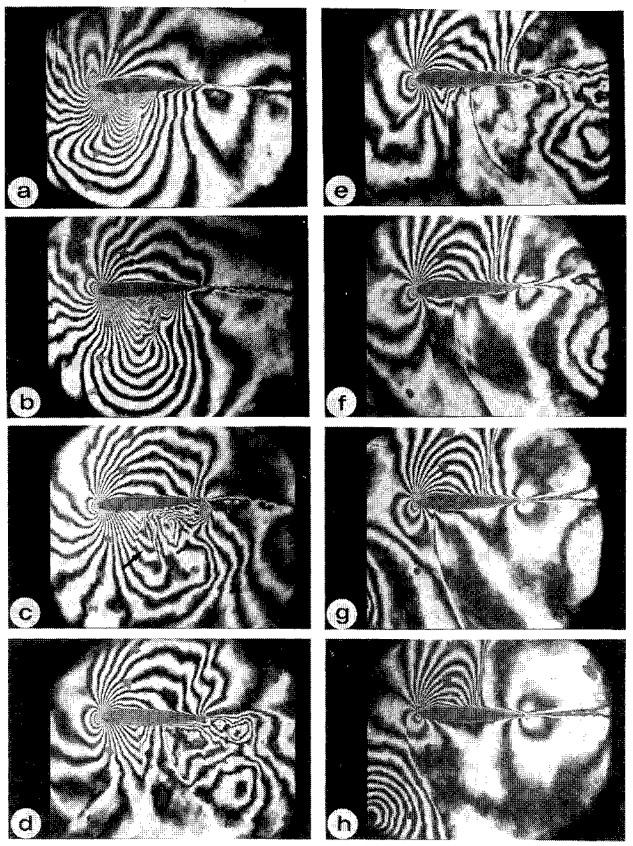

Fig. 8 Transonic waves generated in the wind tunnel. NACA 0012 airfoil, $M = 0.81$, $\Gamma = 24$ m²/s, $c = 120$ m, and a framing rate 10 kHz. The arrow in (c) indicates the cascade of shock waves.

confined supersonic flow region occurs. A typical example is shown in Fig. 8.

When a clockwise-rotating vortex approaches an airfoil the stagnation point moves upward (Fig. 8a). Below the airfoil one sees a locally confined supersonic flow region terminated by a shock wave which will propagate upstream when the vortex has passed the supersonic region (Figs. 8d–h). In some cases, not only single shock waves, but even cascades of shocks (Fig. 8c) which merge to a single wave when they move upstream, were found. A convincing explanation for the occurrence of the cascade instead of a simple shock wave could not yet be found.

To improve the understanding of transonic waves, the flow Mach number, the circulation of the incoming vortex, and its lateral distance to the airfoil have been varied. In Sec. IV.A. these data will be compared with some theoretical estimations.

IV. Theoretical Models

What has been described qualitatively above was also studied in detail by variation of the parameters involved. This gives us criteria for the occurrence and some data for the strength of transonic and compressibility waves.

A. Transonic Waves

From a very simplified point of view (which accounts only partly for compressibility effects) one might expect that transonic waves occur if

$$v_{\text{total}} = v_{\text{mean, profile}} + \frac{\Gamma}{\pi y_0} > c_0$$

is fulfilled.[20] Here, $v_{\text{mean, profile}}$ is the maximum velocity at the shoulder of the airfoil in a steady flow without vortices, Γ is the circulation of the vortex, y_0 is the distance between vortex and airfoil normal to flow direction, and c_0 is the speed of

sound. Here the second term on the right side accounts for the real vortex and is approximate for a mirror vortex to comply with the boundary condition at the airfoil. This very simple estimation has been confirmed experimentally as can be seen from Fig. 9. Unfortunately, an estimation of the strength of the transonic waves could not be given yet.

B. Compressibility Waves

A very simplified model has been developed for the description of compressibility waves.[20] It is based on the assumption of the existence of a piston-like source at the leading edge of the airfoil. In order to fulfill the boundary condition $v_{\text{normal}} = 0$, it is required that the velocity induced at the surface of the airfoil be compensated by the piston source. Therefore, this piston velocity has to be

$$v_{\text{piston}} = -\frac{\Gamma}{2\pi y_0}$$

If the impedance at the airfoil is given by $I = \rho_0 c_0$, one gets for the radiated pressure field

$$p = \frac{\rho_0 c_0 \Gamma}{2\pi y_0}\sqrt{\frac{d}{2\pi R}}\sqrt{\frac{1}{1 - M\cos\alpha}}$$

which includes also the Doppler effect. Here, ρ_0 is the density, c_0 is the speed of sound, Γ is the circulation of the oncoming vortex, y_0 is the distance between the vortex and the airfoil normal to the flow direction, d is the thickness of the profile, R is the distance to the observation point, and α is the observation angle with respect to the mean flow direction.

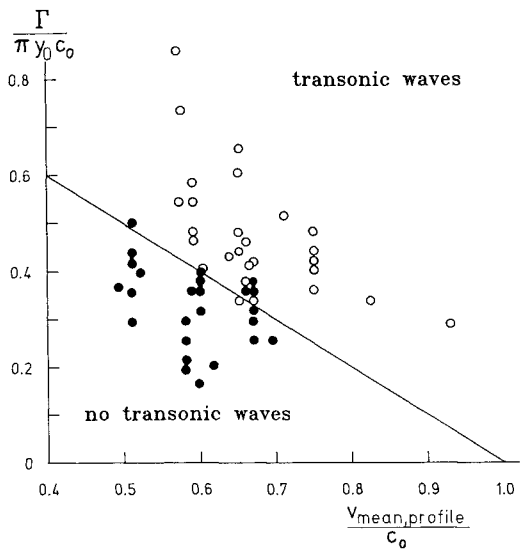

Fig. 9 Transonic waves: A comparison between experimental data and the theoretical prediction.

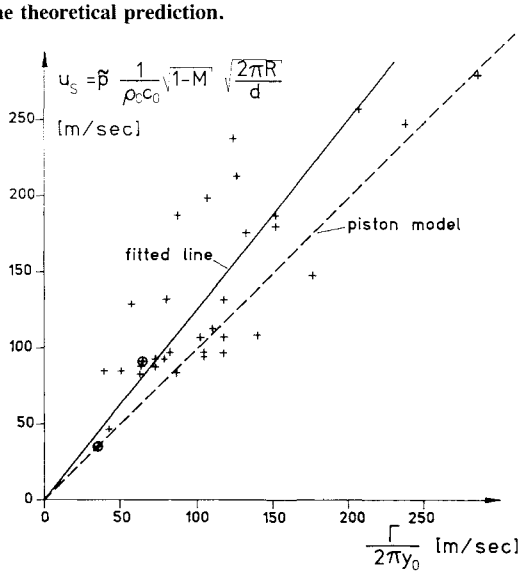

Fig. 10 Piston model: Vortex-induced velocity compared with a piston source velocity.

A comparison of the acoustic particle velocity, estimated by the model, and the acoustic particle velocity, obtained from pressure data from the interferograms, is shown in Fig. 10. The solid line represents a least-square fit to the experimental data and the dashed line describes the estimation by the simplified piston theory. The general trends of both results agrees, but there is a systematic deviation of about 30%.

V. Conclusion

Experiments to visualize and help understand the transonic vortex-airfoil interaction were performed. For this purpose two-dimensional model flows were investigated by interferometric techniques and pressure measurements. The experiments were performed in two different experimental facilities. In the first series of experiments the interaction of an airfoil with vortices of an von Kármán vortex street generated in a transonic wind tunnel was studied. The second series of experiments were conducted in a special shock tube where the starting vortex behind a lifting airfoil was used to study the BVI.

Two different kinds of sound waves were identified which (at least to our knowledge) have not been discussed before. They have been called transonic waves and compressibility waves. Both are different from the sound waves due to ordinary subsonic noise generation.

Unfortunately, due to experimental limitations, the directivity patterns of the two sound waves could not be measured accurately enough to derive prediction schemes for the application to real helicopter noise. Improved experiments and data evaluation methods should help to overcome these shortcomings in the future.

References

[1]Schmitz, F. H., and Yu, Y. H., "Helicopter Impulsive Noise: Theoretical and Experimental Status," *Journal of Sound and Vibration*, Vol. 109, No. 3, 1986, pp. 361–422.

[2]Möhring, W., Müller, E.-A., and Obermeier, F., "Problems in Flow Acoustics," *Reviews of Modern Physics*, Vol. 55, No. 3, 1983, pp. 707–724.

[3]Ffowcs Williams, J. E., and Hawkings, D. C., "Sound Generation by Turbulence and Surfaces in Arbitrary Motion," *Philosophical Transactions of the Royal Society of London, Series A*, Vol. 264, No. 1151, 1969, pp. 321–342.

[4]Möhring, W. F., Müller, E.-A., and Obermeier, F. F., "Schallerzeugung durch instationäre Strömung als singuläres Strömungsproblem," *Acustica*, Vol. 21, No. 3, 1969, pp. 184–188.

[5]Srinivasan, G. R., McCroskey, W. J., and Baeder, J. D., "Aerodynamics of Two-Dimensional Blade-Vortex-Interaction," AIAA 18th Fluid Dynamics and Plasmadynamics and Lasers Conf., AIAA Paper 85-1560, Cincinnati, OH, July 1985.

[6]Rai, M. M., "Navier-Stokes Simulations of Blade-Vortex-Interaction Using High-Order Accurate Upwind Schemes," AIAA 25th Aerospace Sciences Meeting, AIAA Paper 87-0543, Reno, NV, Jan. 1987.

[7]Ballmann, J., and Kocaaydin, C. S., "Some Aerodynamic Mechanisms of Impulsive Noise During Blade-Vortex-Interaction," 16th European Rotorcraft Forum, 8th European Helicopter Association Symposium, Paper II10, Glasgow, Sept. 18–21, 1990, pp. II.10.1.1–10.1.14.

[8]Ehrenfried, K., "Numerische Untersuchung von Wirbel-Tragflügel-Wechselwirkungen im Transsonischen Geschwindigkeitsbereich," Max-Planck-Institut für Strömungsforschung, Göttingen, Germany, Bericht 8/1991.

[9]Caradonna, F. X., Laub, G. H., and Tung, C., "An Experimental Investigation of the Parallel Blade-Vortex-Interaction," 10th European Rotorcraft Forum, Paper 4, The Hague, The Netherlands, Aug. 1984.

[10]Haertig, J., Johe, C., and Gnemmi, P., "Experimental Investigation of a 2D Parallel Vortex/Airfoil Interaction," *Laser Anemometry and Applications*, edited by A. Dybbs, Vol. II, The American Society of Mechanical Engineering, Cleveland, OH, Aug. 1991, pp. 413–424.

[11]Meier, G. E. A., and Timm R., "Unsteady Vortex Airfoil Interaction," *AGARD Conference Proceedings*, Vol. 386, 1985, pp. 16:1–16:10.

[12]Mandella, M., and Bershader, D., "Quantitative Study of the Compressible Vortex-Generation, Structure and Interaction with Airfoils," AIAA Paper 87-0328, Reno, NV, 1987.

[13]Obermeier, F., "Sound Generation by Rotor-Vortex-Interaction in Subsonic Flow," AIAA Paper 90-3974, Tallahassee, FL, Oct. 1990.

[14]Zhang, K. Y., Lent, H.-M., and Meier, G. E. A., "Experimental Investigation of a Counter Rotational Vortex-to-Wedge Interaction and Generation of a New Wave," Deutsche Forchungsanstalt für Luft-und Raumfahrt, Rept.: IB 222-90A37, Göttingen, Germany, Sept. 1990.

[15]Meier, G. E. A., Lent, H.-M., and Löhr, K. F., "Sound Generation and Flow Interaction of Vortices with an Airfoil and a Flat Plate in Transonic Flow," *Fluid Dynamics Research*, Vol. 3, 1988, pp. 344–348.

[16]Lent, H.-M., Löhr, K. F., Meier, G. E. A., and Schievelbusch, U., "Some Processes of Sound Generation in a Vortex-Airfoil System with Parallel Axes," *Journal d'Acoustique*, Vol. 2, Dec. 1989, pp. 365–367.

[17]Bretthauer, B., Meier, G. E. A., and Stasicki, B., "An Electronic Cranz-Schardin Camera," *Review of Scientific Instruments*, Vol. 62, No. 2, 1991, pp. 364–368.

[18]Parker, R., "Resonant Effects in Wake Shedding from Parallel Plates: Some Experimental Observations," *Journal of Sound and Vibration*, Vol. 4, No. 1, 1966, pp. 62–72.

[19]Parker, R., "Resonant Effects in Wake Shedding from Parallel Plates: Calculation of Resonant Frequencies," *Journal of Sound and Vibration*, Vol. 5, No. 2, 1967, pp. 330–343.

[20]Lent, H.-M., "Modell für die Schallentstehung bei kompressibler Wirbel-Körper-Wechselwirkung," Mitteilungen aus dem Max-Planck-Institut für Strömungsforschung, Nr. 96, Göttingen, Germany, 1990.

[21]Bartels, H.-H., Bretthauer, B., Meier, G. E. A., and Wenskus, R., "Quantitative Interferometrie," 2D-Meßtechnik, DGLR Bericht 88-04, Markdorf, Germany, 1988, pp. 5–23.